

Optical Measurements of Cavitation in Tribological Contacts

This content has been downloaded from IOPscience. Please scroll down to see the full text.

2015 J. Phys.: Conf. Ser. 656 012119

(<http://iopscience.iop.org/1742-6596/656/1/012119>)

View [the table of contents for this issue](#), or go to the [journal homepage](#) for more

Download details:

IP Address: 131.231.136.80

This content was downloaded on 09/12/2015 at 16:15

Please note that [terms and conditions apply](#).

Optical Measurements of Cavitation in Tribological Contacts

Tian Tang, Nick Morris and Jeremy Coupland

Department of Mechanical and Manufacturing Engineering, Loughborough
University, UK

E-mail: T.Tang2@lboro.ac.uk

Abstract. The paper describes the use of a white light interferometer to measure the cavitation bubble and oil film thickness in a tribological contact and compares the results to theory. It is found that oil film thickness is best predicted by the theory proposed by Coyne and Elrod.

1. Introduction

The role of cavitation in tribological contacts has been discussed by many authors with regard to load capacity, lubricant thickness, frictional losses and wear in sliding or rolling contact bearings [1-15]. The pioneering work of Osborne Reynolds in 1886 showed that the lubricant pressure distribution along a smooth sliding bearing can be expressed by the equation that now bears his name,

$$\frac{\partial}{\partial x} \left(h^3 \frac{\partial p}{\partial x} \right) = 6\eta U \frac{\partial h}{\partial x} \quad (1)$$

where $h(x)$ is the height profile, $p(x)$ is the oil film pressure, η is the lubricant viscosity and U is the bearing sliding velocity [1]. For the case of a convergent/divergent tribological contact the solution to this equation predicts a significant increase in gauge pressure within the converging section followed by a decrease in pressure (within the diverging section) that often falls below the saturation or vapor pressure which signifies the onset of cavitation or film rupture. The cavitation, however, clearly modifies the flow and must be properly accounted for in the theory using appropriate boundary conditions.

The first cavitation model was introduced by Gumbel [2] who assumed that film rupture occurred at the beginning of the divergent region. Swift [3] and Stieber [4] introduced an improved model assuming the pressure gradient equal to zero at the film rupture position. In order for the flow to exit the contact it must either pass around multiple cavitation bubbles or flow over (or under) a single cavity. These two theories have been studied extensively but separately. The assumption of flow around multiple cavitation bubbles has been studied by Floberg [5], Jacobson and Floberg [6], Olsson [7] and Floberg [8]. Taken together these works are referred to as JFO theory which not only satisfies mass flow continuity and predicts the film rupture position, but also locates the reformation position and is therefore capable of predicting the load carrying capacity. The theory has widely used after an efficient algorithm for calculation was introduced by Elrod [9, 10] and is now commonly referred to as the Elrod cavitation model.

Alternatively the lubricant can flow over (or indeed under) a single cavity. Prandtl's theory of boundary layers and flow separation was built upon by Birkhoff and Hays [11] to determine that the point at which flow separation will occur due to adverse pressure gradients causing reverse flow in the diverging region of the contact. Coyne and Elrod [12, 13] improved the model by introducing the influence of surface tension, gravity and fluid inertia. In essence, the inclusion of surface tension effects allows the local fluid pressure to drop below the cavity pressure and the point of film rupture moving further along the divergent section.



Both the assumption of flow around multiple cavitation bubbles and the assumption of flow over a single cavitation bubble are supported to a certain degree by experimental observation. Dowson [14] shows the flow between multiple cavitation bubbles generated in the lubricant flow between a sliding surface and a fixed convex surface. On the other hand, Heshmat [15] photographed the cavitation generated by a flat stationary surface and a rotating cylindrical surface showing flow between a single bubble and the rotating surface.

In a previous paper we have investigated the lubricant flow in a glass sliding bearing (modelling a ring-cylinder liner conjunction) using a digital holographic microscope [16]. In essence this transmission setup measures the phase and amplitude of the wavefront passing through the tribological contact. This information allowed the computation of high resolution images of the cavitation bubbles and, by comparing wavefronts before and after the onset of cavitation, high fidelity quantitative measurements of the bubble thickness are possible. Although the measurements clearly show multiple cavitation bubbles and suggest that the bubbles only contact the cylindrical surface, the transmission setup does not allow the oil film thickness to be measured. In this paper, we report an interferometric reflection geometry using white light to measure both the bubble and the film thickness. Measurement results are discussed and compared with the theoretical models of lubricant flows.

2. Experimental configuration

The contact consists of a plane glass surface and a cylindrical lens as shown in figure 1. The plane glass is driven by a bidirectional motorized translation stage with controlled speed up to 2.3 mm/s . The cylindrical lens (radius= 13.25 mm , width= 12.5 mm and length= 25 mm) is fixed on a stationary metal surface. The lubricant oil between the two bearing surface is additive-free, classic green gear oil with a viscosity $\eta = 1.508 \text{ Pa}\cdot\text{s}$ measured at room temperature (20 C°). The sliding plane glass is entirely supported by the hydrodynamic film with a constant load of $W = 2.65 \text{ N}$. In this experiment the bearing surfaces are constructed from high refractive index S-NF57 glass ($n = 1.84$) which, relative to the refractive index of the oil ($n = 1.49$), provides sufficient reflected light. The white light interferometer configuration is shown in figure 2.

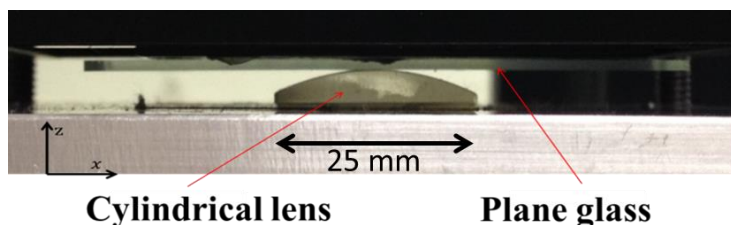


Figure 1. Glass bearing configuration.

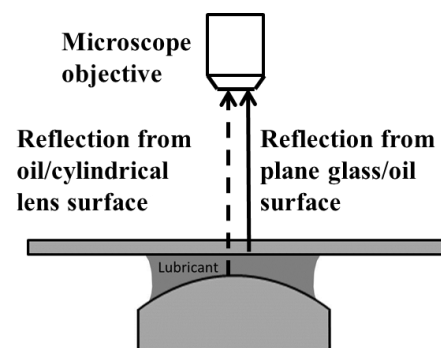


Figure 2. White light interferometer.

In this configuration as the illumination passes through the bearing, a reflection occurs at the interface between the plane glass and oil and another at the interface between the oil and cylindrical surface. Since the illumination is white light, interference is observed only if these surfaces are in close proximity as shown in figure 3. Using white light interferometry, the minimum thickness can be found unambiguously by using a theoretical model to fit the experiment results as follows.

3. Analysis

To a good approximation the intensity of two reflections interference, I , can be expressed as a function of the thickness profile, $h(x)$, such that,

$$I = I_1 - I_2 \cos\left(\frac{4\pi}{\lambda} h(x)\right) E(h(x)) \quad (2)$$

where I_1 and I_2 are constants, λ is the average wavelength and E is a function that describes the fringe envelope. Since the thickness profile is known, the thickness of the oil film $h(x)$, can be expressed as a function of position x ,

$$h(x) = h_0 + R(1 - \cos(\arcsin(\frac{x}{R}))) \quad (3)$$

where h_0 is the minimum thickness and R is the radius of cylindrical lens. Using this equation the values of the constants in equation 2 together with the fringe envelope function can be found by analyzing an interferogram taken when the bearing is stationary. When driven, the oil film thickness can then be found by iteratively searching for h_0 . Using data up to the point of film rupture the normalised fringe data ($I_{norm} = (I - I_1)/I_2$) is shown in figure 4. Note the origin in figure 4 is $x = 336 \mu\text{m}$ in figure 3. Here, the blue line represents the average normalized intensity while the red line is that predicted by equation 2. A similar method can be used to measure the thickness of the bubble

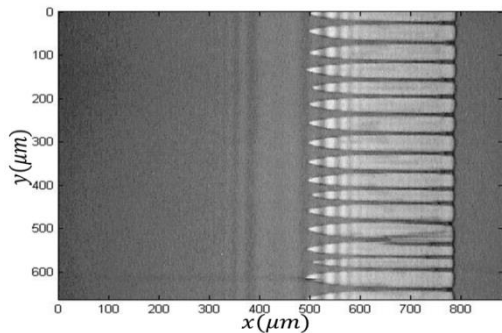


Figure 3. White light interferogram.

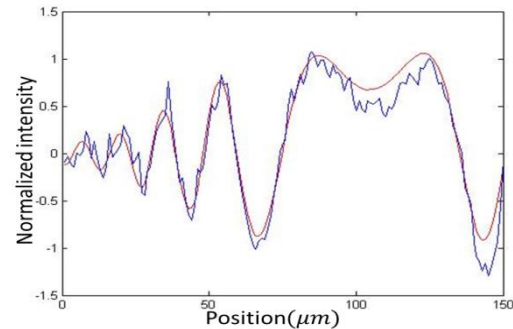


Figure 4. Average normalized intensity (blue) and theoretical fit (red).

4. Results

The reflection geometry has been used to measure the minimum thickness, bubble position and bubble thickness at various speeds (table 1) and has been compared with those predicted by the model discussed in section 1.

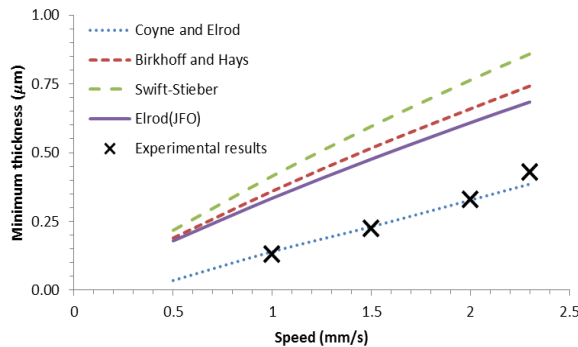


Figure 5 Minimum thickness versus speed.

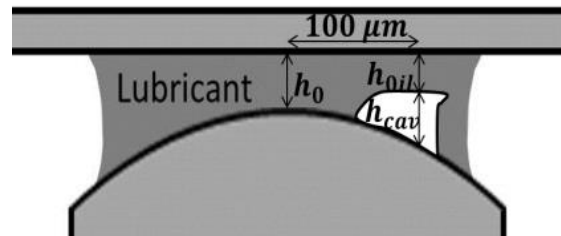


Figure 6 Bubble geometry.

Figure 5 shows a comparison of the measured minimum film thickness as a function of entrainment speed with those predicted by the different theoretical models. It can be seen that although there are clearly multiple bubbles (as figure 3) the minimum film thickness is best predicted by the Coyne and Elrod model that assumes flow over a single bubble.

Table 1 Bubble thickness and oil film thickness at $100 \mu\text{m}$ at different speeds

Speed (mm/s)	h_{cav} (μm)	h_{oil} (μm)	h_0 (μm)
1.0	0.2835	0.3092	0.149
1.5	0.3982	0.2902	0.256
2.0	0.506	0.285	0.359
2.3	0.5566	0.301	0.426

Since we measure both the position of the glass surfaces and the bubble thickness, the oil film thickness over the cavitation bubbles can also be calculated. With reference to figure 6 these quantities are tabulated in Table 1. It can be seen that with the increase of entrainment speed, the minimum film

thickness and bubble thickness will increase; however, the oil film that flows over the bubbles is of almost constant thickness.

5. Conclusions

This paper has introduced a white light interferometer and associated analysis methods as an aid to understanding cavitation in tribological contacts. Using this approach we have been able to measure oil film and bubble thickness simultaneously and can compare these results with those predicted by theory. Although the results clearly show multiple bubbles (as figure 3) the minimum film thickness is best predicted by the Coyne and Elrod model that assumes flow over a single bubble. We have verified that the oil film does indeed flow over the bubbles and furthermore we have shown that the thickness of this component (approximately 300 nm) is almost independent of entrainment velocity.

It is evident that neither the multiple bubble (JFO, Elrod) nor single bubble (Elrod and Coyne) models fully explain real cavitation, at least in the lightly loaded flow conditions studied here. It is clear that aspects of both theories are necessary to properly predict the pressure boundary conditions and hence calculate the load conditions. Furthermore it is expected that surface roughness will strongly affect bearings performance and further work is planned to study its effect using interferometry.

References

- [1] Reynolds O 1886 On the theory of lubrication and its application to Beauchamp Tower's experiments including an experimental determination of the viscosity of olive oil *Philos. Trans. R. Soc. London Ser. A* 177, 157-233
- [2] Gümbel L K R 1921 Vergleich der Ergebrusse der rectinerischen Behandlung des Lagerschmierangspromblem mitneueren Versuchsergebrussen *Monatsbl. Berliner Bez Ver. Dtsch. Ing.* 125-128
- [3] Swift W 1933 The stability of lubricating film in journal bearing *J. Inst. Civ. Eng.* 233 (1), 267-88
- [4] Stieber W 1933 *Das Schwimmlager. Berlin: Ver. Dtsch. Ing*
- [5] Floberg L 1973 On journal bearing lubrication considering the tensile strength of the liquid lubricant. *Transactions of the Machine Elements Division, Lund Technical University, Lund, Sweden* 1-26
- [6] Jakobson B and Floberg L 1957 The finite journal bearing considering vaporization. *Transactions of Chalmers University Technology, Goteborg, Sweden* 190, 1-119
- [7] Olsson K O 1965 Cavitation in dynamically loaded bearings *Transactions of Chalmers University Technology, Goteborg, Sweden* 308
- [8] Floberg L 1974 Cavitation boundary conditions with regard to the number of streamers and tensile strength of the liquid *Cavitation and related phenomena in lubrication, Proceedings of the 1st Leeds-Lyon Symposium on Tribology, University of Leeds, Leeds, UK* 31-36
- [9] Elrod H G and Adams M 1974 A computer program for cavitation and starvation problems *Cavitation and related phenomena in lubrication* 37-41
- [10] Elrod H G 1981 A cavitation algorithm *Journal of Tribology* 103(3), 350-354
- [11] Birkhoff G and Hays D F 1963 Free boundaries in partial lubrication *Journal of Mathematics and Physics* 42(2), 126
- [12] Coyne J C and Elrod H G 1970 Conditions for the rupture of a lubricating film. Part I: theoretical model *Journal of Tribology* 92(3), 451-456
- [13] Coyne J and Elrod H G 1971 Condition for the Rupture of a Lubricating Film-Part II: New Boundary condition for Reynolds Equation *Journal of Lubrication Technology* 93, 156
- [14] Dowson D 1957 Cavitation in lubricating films supporting small loads *Proc. Inst. Mech. Eng. Conf. Lubr. Wear.* 93-99
- [15] Heshmat H 1991 The mechanism of cavitation in hydrodynamic lubrication. *Tribology transactions* 34(2), 177-186
- [16] Tang T, Morris N, Coupland J, and Arevalo L 2015 Cavitation Bubble Measurement in Tribological Contacts Using Digital Holographic Microscopy *Tribology Letters* 58(1), 1-10